International Geology Review, Vol. 40, 1998, p. 945–962.
Copyright © 1998 by V.H. Winston & Son, Inc. All rights reserved.

Exploring the Complexities of the Serenitatis Basin: Breccia Clasts from Apollo 17

CLIVE R. NEAL

Department of Civil Engineering and Geological Sciences, University of Notre Dame, Notre Dame, Indiana 46556-0767

AND LAWRENCE A. TAYLOR

Planetary Geosciences Institute, Department of Geological Sciences, University of Tennessee, Knoxville, Tennessee 37996-1410

Abstract

Thirteen new breccia clasts of highland lithologies are described from the Apollo 17 site. The clasts were extracted from three breccias: two from sample 73215 (aphanitic impact melt breccia), six from 73216 (impact melt breccia), and five from 77035 (micropoikilitic impact melt breccia). Breccias 73215 and 73216 were collected from the rim of a 10 m crater at Station 3 and breccia 77035 was collected at Station 7 at the base of the North Massif. The clasts are subdivided into melt-free and melt-rich groups. The melt-free clasts include pristine and brecciated lithologies, with one pristine gabbronoritic anorthosite containing 15 ppb Ir. The melt-rich clasts have compositions that are similar to LKFM, rather than to Apollo 17 KREEP basalts described as clasts from breccia 72275 by Salpas et al. (1987). Three main conclusions are drawn from this study: (1) the presence of 15 ppb Ir in a pristine gabbronoritic anorthosite further demonstrates the complexities associated with estimating the highly siderophile element content of the lunar crust and siderophile element abundances cannot be used in isolation to demonstrate pristinity (or lack thereof); (2) the KREEP basalts from breccia 72275 probably are not indigenous to the Serenitatis Basin and were transported to the Apollo 17 site by impact processes. Apollo 17 KREEP is in reality LKFM in composition; and (3) the "cryptic" component required to define KREEPy LKFM impact compositions probably will never be defined mineralogically. This component was derived from the final liquid to crystallize from fractional crystallization of either an Mg-suite pluton or the lunar magma ocean. Consequently, this component will easily melt when disrupted by large impacts and now is present as glass in breccia matrixes and/or as grain boundary films.

Introduction

IN MOST models of lunar evolution, the highlands region represents ancient plagioclase-flotation cumulate crust from the lunar magma ocean (LMO), with complementary mafic cumulates forming the mantle (e.g., Smith et al., 1970; Taylor and Jâkes, 1974; Warren, 1985). The lack of atmosphere and water on the Moon means chemical weathering of these ancient samples is nonexistent, but they have been exposed to meteorite bombardment that has mechanically mixed, brecciated, metamorphosed, and melted the highlands. Although this bombardment may have been most intense early in the history of the Moon (e.g., Ryder, 1990) and has since tailed off in magnitude since ~3.8 to 3.9 Ga, such meteorite impacts have at least partially obscured our view of the early lunar crust. However, within the returned sample collection, the study of highlands lithologies has revealed important information about impact processes as well as early crustal formation and processes (e.g., Warren et al., 1991).

The focus of this paper is on clasts extracted from three Apollo 17 breccias—samples 73215 (aphanitic impact melt breccia), 73216 (impact melt breccia), and 77035 (micropoikilitic impact melt breccia). It examines a suite of clasts extracted from Apollo 17 breccias to examine both monomict pristine and polymict clasts in order to further explore the geology of the Apollo 17 site. Breccias 73215 and 73216 were collected from the rim of a crater of 10 m diameter at Station 3, and both are impact-melt breccias with entrained lithic clasts. Breccia 77035 was collected at Station 7 at the base of the North Massif, and is a micropoikilitic impact-melt breccia that has partially dissolved the original clasts or welded them into a recrystallized matrix. This has

0020-6814/98/358/945-18 $10.00

produced a very tough rock, from which the entrained clasts are difficult to extract. Previous work on Apollo 17 breccias demonstrated the importance of such studies in enhancing our knowledge of lunar rock types and processes. For example, consortium studies of breccias 73215 and 73255 noted the existence of felsites and high-alumina, VLT-type mare basalts at the Apollo 17 site (e.g., James et al., 1975; Ryder et al., 1975; James and Hammarstrom, 1977; Blanchard et al., 1977; Blanchard and Budahn, 1979; James and McGee, 1980). Although ferroan anorthosite (FAN) lithologies are present in the Apollo 17 highlands (Laul et al., 1989; Warren et al., 1991), the predominance of Mg-suite over ferroan lithologies around the Serenitatis Basin has been documented (e.g., Warren et al., 1987; Salpas et al., 1988).

TABLE 1. Subsample Numbers for Analyzed Clasts

Breccia	Probe mount	Thin section		INAA
73215	.534	.562	.7001	.579
73215	.539	.563	.7002	.580
73216	.36	.61	.7001	.66
73216	.38	.62	.7002	.67
73216	.42	.63	.7003	.68
73216	.49		.7004	.69
73216	.57	.65	.7005	.70
77035	.172		.7001	.226
77035	.185	.221	.7002	.228
77035	.200		.7003	.229
77035	.201		.7004	.230
77035	.206			.206
77035	.227			.227

Petrography and Mineral Chemistry

A total of 13 clasts were extracted from the three breccias—2 from 73215, 5 from 73216, and 6 from 77035. Petrographic observations of the 13 Apollo 17 highland clasts were made using standard techniques, and initial results of our study were reported by Neal, Taylor et al. (1990b) and Eckert et al. (1991a, 1991b, 1991c). It should be noted that traditional metamorphic terminology often is used to describe these samples in order to convey a sense of texture, not paragenesis. In some cases, three sections are available for certain clasts: one was made at the University of Tennessee and is a thick section, one thin section was made at the Johnson Space Center (JSC) from material not used for instrumental neutron activation analysis (INAA), and another was also made at JSC from the INAA sample itself. The thin sections made from INAA samples are suffixed with the notation "700X." Table 1 correlates these numbers in order to identify sections from individual samples when different facets of their petrology are discussed.[1]

Chemical compositions of the individual minerals were determined with a CAMECA SX-50 electron microprobe at the University of Tennessee. Operating conditions were 15 kV accelerating voltage, 100 μamp filament current, and beam currents of 20 nA for feldspars using a slightly defocused beam, and 30 nA for other phases. Usual counting times were 20 seconds on peak and 20 seconds total on background.

Breccia 73215

73215,534/,562/,7001. This subsample is composed of a granulite clast and dark breccia material. The lighter material represents the plagioclase-rich granulite clast, whereas the darker material is mainly very fine grained (<0.01 mm) breccia matrix. The dark breccia exhibits a general cataclastic texture with a bimodal size distribution. Larger subangular clasts of spinel (0.04–0.12 mm; Mg# = 76–85, 100*(Cr/(Cr+Al)) = 9–11), olivine (0.07–0.66 mm; Fo_{89-92}), low-Ca pyroxene (~0.13 mm; it is enstatitic in composition [Wo_{3-5}], but is relatively Fe rich [Mg# = 44–46]), and plagioclase (0.1–0.3 mm; An_{91-96}) grains are set in a fine-grained, granoblastic groundmass (≤0.02 mm) of predominantly plagioclase with minor low-Ca pyroxene and minor glass, producing a porphyroblastic texture. The granulite clast is mineralogically a troctolitic anorthosite dominated by polygonized plagioclase, forming a granoblastic matrix (generally 0.05 mm); some plagioclase clasts reach 0.5 mm in diameter. Olivine "porphyroblasts" (up to 0.5 mm) appear to be reacting with the plagioclase-rich matrix, but smaller olivines (<0.02 mm) appear to

[1]Full details of the petrography can be found at: http://www.nd.edu/~cneal/A17clasts. Only brief descriptions are presented here.

be in equilibrium with plagioclase. Homogeneous, Ca-rich pyroxene (Wo_{42-44}; Mg# = 60–62) is present, but no orthopyroxene was found.

73215,539/,563/,7002. The thin section made from the INAA sample consists of a myriad of tiny (≤0.05 mm) grains, primarily forsterite-rich olivine (up to 0.25 mm, but generally <0.05 mm), which has a much more restricted range than in the previous two sections (Fo_{89-92}), with significant pyroxene and plagioclase (An_{91-96}). The modal mineralogy (see below) indicates that this material is transitional between a dunite and a troctolite. Unlike sections ,539 and ,563, both orthopyroxene (Wo_{1-8}; Mg# = 92–93) and clinopyroxene (Wo_{40-47}; Mg# = 94–95) are present as minor, discrete grains that display little core-to-rim zonation. Rare Fe-Ni metal also is present (≤0.005 mm). There is no texture, as the "clast" has disaggregated.

Breccia 73216

73216,36/,61/,7001. This is mineralogically a gabbronoritic anorthosite containing interlocking plagioclase (An_{87-95}), and low- and high-Ca pyroxene (≤0.4 mm; for Wo_{4-5} Mg# = 73–78 and for Wo_{38-39} Mg# = 72–78, respectively) in an apparent cumulate texture, with some recrystallized zones evident by triple junctions. Necklaces of olivine (Fo_{91-92}) and pyroxene inclusions (individual grains <0.005 mm) are present in some of the larger plagioclase grains. Disruption of some plagioclase twin lamellae suggests that this clast experienced mild deformation. In the section made from the INAA sample, chips of breccia matrix exhibiting a cataclastic to annealed texture are also present. These breccia chips have a bimodal grain size and an almost porphyroblastic texture, with larger clasts of plagioclase, olivine, and skeletal ilmenite reaching 0.2 mm.

73216,38/,62/,7002. This is a highly brecciated/recrystallized anorthositic gabbronorite with a general annealed granulitic to granoblastic/porphyroblastic texture and a groundmass grain size of ~0.02 mm. The granulite clast is composed primarily of plagioclase (up to 1.5 mm, but usually ~0.3 mm with intergrain variation of An_{95-83}). Mafic minerals are more abundant toward the edges of this clast. Olivine (Fo_{69-71}), orthopyroxene (Wo_{4-5}; Mg# = 74–79) and clinopyroxene (Wo_{29-39}; Mg# = 75–79) rarely reach 0.25 mm and are usually ≤0.04 mm. Matrix material is predominantly plagioclase with subordinate olivine and pyroxene. Devitrified impact melt permeates the breccia matrix and corrodes the larger, predominantly plagioclase crystals.

73216,42/,63/,7003. This is a devitrified impact melt made up predominantly of acicular plagioclase crystals forming a variolitic texture. The radiating plagioclase masses reach 0.2 mm in diameter. Rare plagioclase grains exhibit slight core-to-rim zonation (An_{92} to An_{87}), and the overall inter-grain variation is An_{85-94}. Ilmenite reaches 0.5 mm in length, although smaller (0.04–0.1 mm) ilmenites are more abundant, and contain rutile and spinel exsolution features. The larger ilmenites tend to cut across the variolitic plagioclase, and armalcolite (≤0.18 mm) forms the cores to these grains. Ilmenite and armalcolite possess relatively high Mg#s (23–31 and 45–48, respectively). Pyroxene and olivine occur as discrete grains (up to 0.25 mm) or as necklaces up to 1.5 mm long composed of small (≤0.05 mm) grains. Both low- and high-Ca pyroxenes are present. Low-Ca pyroxene is enstatitic (Wo_{4-5}) and high-Ca pyroxene is augite (Wo_{39-40}); both have similar Mg#s (74–77 and 77–78, respectively) (Table 1). Olivine (Fo_{66-68}) forms ≈0.005 mm cores to some of the larger pyroxenes, but also occurs as small (≤20 μm), round, discrete grains; a small inclusion in ilmenite has a slightly more forsteritic composition of Fo_{73-74}.

73216,49/,7004. This is a recrystallized norite with a cataclastic to granoblastic-annealed texture. The thin section made from the INAA sample contains nine chips ranging from polygonal plagioclase to granulitic and cataclastic breccia. Two chips are comprised entirely of polygonal plagioclase, with individual grains reaching 0.5 mm. Some of this material adheres to a breccia chip. Plagioclase exhibits discontinuous core-to-rim zonation (cores = An_{93-96}; rims = An_{83-87}), and strained extinction. The breccia has an overall granoblastic to granulitic texture with porphyroblasts of plagioclase, skeletal ilmenite, and low-Ca pyroxene (0.2–0.5 mm). Impact melt permeates the breccia matrix and clast. This melt has devitrified, yielding predominantly variolitic plagioclase with subordinate ilmenite (Mg# = 24–31) and armalcolite (Mg# = 46–59) (all are ≤0.01 mm). Semi-opaque glassy areas still are present, but never exceed 1 mm.

73216,57/,65/,7005. This is a gabbronoritic

anorthosite exhibiting a striking orthocumulate texture with intercumulus pyroxenes (up to 0.8 mm) set in cumulus plagioclase. Cumulus plagioclase ranges from subequant grains (1.06–1.55 mm) to laths (0.12–0.35 mm). It exhibits slight discontinuous core-to-rim zonation from cores of An_{98} to rims of An_{93}. No olivine was observed. Both high-Ca (~0.75 mm; Wo_{39-41}, Mg# = 78–79) and low-Ca pyroxene masses (~0.2–0.3 mm; Wo_{4-5}, Mg# = 75–76) are present. Exsolution lamellae are abundant in the pyroxenes, indicating a slow cooling formational environment. The texture indicates that the initial accumulation of plagioclase was followed by crystallization of intercumulus pyroxenes, late-stage metal, and ilmenite.

Breccia 77035

77035,172/,7001. This is a dunite, with the section made from the INAA sample containing six olivine grains of homogeneous composition (Fo_{88-89}), although discontinuous rims (30–50 μm) of Fo_{80} are present on two of the crystals. No adhering breccia matrix is present in this section, although there is in ,172. The breccia matrix is cataclastic to granoblastic and is plagioclase and ilmenite rich; subordinate olivine and pyroxene also are present, with matrix grain sizes up to 0.05 mm. Porphyroblasts of plagioclase (up to 0.4 mm) are present. The olivine clast has small (<5 μm) spinel inclusions.

77035,185/,221/,7002. This clast is of an impact melt containing primarily opaque impact glass, within which are grains of fractured and partially annealed, essentially homogeneous plagioclase (An_{92-94}) and orthopyroxene grains (Wo_{3-5}; Mg# = 78–79). The general texture is cataclastic, bordering upon vitrophyric. Plagioclase and orthopyroxene reach 0.5 mm. The larger plagioclase crystals are disintegrating and appear to be partly assimilated by the glass. The larger pyroxene grains exhibit a reaction rim.

77035,200/,7003. The thin section made from the INAA sample contains no adhering breccia matrix. This sample is a gabbroic anorthosite clast consisting of equigranular (0.4 mm) polygonized plagioclase (An_{85-87}) in a granoblastic texture. Grain boundaries are curved and meet at triple junctions. Minor olivine (up to 0.2 mm; Fo_{69-73}), clinopyroxene (0.6 mm; Wo_{42-44}; Mg# = 77–79), and orthopyroxene (0.2 mm; Wo_{2-4}; Mg# = 79–83) are present, but the section is dominated by plagioclase (>80%). Small (<0.01 mm) mafic mineral inclusions are present in plagioclase, and one, possibly two, fractured zircons ≈0.05 mm in length are present along the grain boundaries of plagioclase. Two areas within this clast exhibit melting and brecciation features.

77035,201/,7004. This clast is a heavily brecciated gabbroic anorthosite that has been welded together by an opaque glass. The glass occurs in veins through the clast (~0.05 mm wide) and is ubiquitous along grain boundaries. The clast contains predominantly plagioclase (up to 0.8 mm; An_{93-96}), ilmenite (up to 0.2 mm; Mg# = 19–23), and pyroxene (up to 0.5 mm; zonations from pigeonite cores [Wo_{13}; Mg# = 74] to augite rims [Wo_{42}; Mg# = 79]). Olivine (Fo_{68-70}) forms a relatively minor phase and never exceeds 0.1 mm.

77035,206. An overall cataclastic to annealed texture is evident in this anorthositic gabbronorite, with porphyroblasts of plagioclase (An_{93-96}) grains (up to 0.9 mm) set in a recrystallized, granoblastic to granulitic matrix (<0.1 mm) dominated by plagioclase of the same composition. Several pyroxene porphyroblasts appear to contain minute whitlockite inclusions (<0.005 mm). Low-Ca pyroxene (<0.1 mm; Wo_4, Mg# = 76), high-Ca pyroxene (Wo_{37-39}; Mg# = 77–79), olivine (<0.05 mm; Fo_{71-74}), ilmenite (~0.05 mm; Mg# = 19–25; MgO = 5–6 wt%), and Fe-Ni metal (<0.005 mm) also are present within and distributed throughout the matrix.

77035,227. The general texture of this devitrified impact melt is equigranular to sub-variolitic. Relict xenocrysts of subrounded plagioclase (up to 0.45 mm) and low-Ca pyroxene (up to 0.14 mm) are present in a recrystallized matrix (<0.1 mm) of plagioclase (An_{70-96}), olivine (Fo_{70-74}), low-Ca pyroxene (Wo_{3-6}; Mg# = 70–81), ilmenite (Mg# = 18–20), Fe-Ni metal, and troilite.

Whole-Rock Chemistry

Whole-rock compositions were determined by instrumental neutron activation analysis at Oregon State University (see Hughes et al., 1988 for analytical details). The largest possible sample weights were used for INAA in order to obtain a representative analysis for each clast. Compositions are presented in Table 2 along with the relative uncertainties associated with the analyses. Chondrite-normalized profiles are used to repre-

TABLE 2. Ranges of Mineral Compositions in the Apollo 17 Clasts

Clast no.	Olivine Fo	Plag. An	Low-Ca Px Wo	Low-Ca Px En	Low-Ca Px Mg#	High-Ca Px Wo	High-Ca Px En	High-Ca Px Mg#	Ilm. Mg#	Armal. Mg#	Spinel Cr#	Spinel Mg#	Metal Ni:Co
							73215						
,534	89–92	91–96	3–5	42–44	44–46	40–42	34–35	56–59	—	—	9–11	76–85	—
,539	74–92	90–97	1–8	68–88	71–93	40–47	53–55	93–95	—	—	10–11	74–77	—
							73216						
,36	91–92	87–95	4–5	70–72	73–78	38–39	47–48	72–78	20–23	—	—	—	7–11
,38	69–75	83–95	4–5	70–74	74–79	29–39	47–53	75–79	18–26	—	—	—	3–7
,42	66–74	78–93	4–5	71–74	74–77	39–40	46–48	77–78	23–31	45–48	—	—	9–26
,49	68–70	83–96	4–5	70–75	74–79	39–40	46–47	77–81	24–31	46–59	—	—	9–11
,57	—	93–98	4–5	71–73	75–76	39–41	46–47	78–79	24–25	—	—	—	12–16
							77035						
,172	80–89	—	—	—	—	—	—	—	—	—	—	—	—
,185	—	92–94	3–5	74–76	78–79	—	—	—	—	—	—	—	—
,200	69–73	85–91	—	—	—	13–44	45–68	74–79	—	—	—	—	8–10
,201	68–70	93–96	3–5	65–76	68–78	27–36	49–58	77–82	19–23	—	—	—	6–12
,206	71–74	93–96	4	73	76	37–39	47–49	77–79	19–25	—	—	—	7–11
,227	70–74	76–96	3–6	67–78	70–81	—	—	—	18–20	—	—	—	12–16

sent the trace-element data of these clasts and to compare them to Apollo 17 KREEP (Salpas et al., 1987) and Apollo 17 highlands lithologies (72415/7 dunite [Laul and Schmit, 1975; Ryder, 1992], 77215 Mg-norite [Winzer et al., 1974, 1977], 76535 Mg-troctolite [Rhodes et al., 1974; Haskin et al., 1974; Weismann and Hubbard, 1975]). Furthermore, the clasts studied here have been subdivided into two groups—those that contain or are impact melts, and those that essentially are melt free.

A word of caution is warranted regarding the Hf and Au abundances. Determinations for Hf by INAA are very precise (generally 2 to 10%). All analyzed clasts display positive Hf anomalies when normalized to chondritic meteorites, but this anomaly is not present in the data of other Apollo 17 samples used for comparison, suggesting that these data should be viewed as an upper limit for Hf concentrations. Gold has been detected in all clasts analyzed, whereas Ir has been found only in three. The sensitivity for Ir generally is the same as for Au when analyzed by INAA (see Table 3). Two possibilities exist for the occurrence of Au in these samples: (1) contamination, or (2) the correction on the 412 keV peak of ^{198}Au was not made from the 411 keV peak of ^{152}Eu. Although the "rough pickings" were performed at the University of Tennessee, every effort was made to ensure that contamination was averted. Picking was conducted using plastic tongs and spatulas in a clean area; analysts removed all jewelry and washed their hands prior to handling the samples. It is not known if the required correction was made to the INAA data. The conclusion that we will make is that the reported gold abundances probably are not indigenous to the samples.

Melt-free clasts

Seven of the 13 clasts studied are essentially free of injected melt although several have been brecciated; 77035,229(,200/,7003) contains melt that appears to be derived from the clast itself. Major-element abundances are generally similar to those of the clasts containing impact melts, but they have generally lower K_2O abundances (Figs. 1A and 1B; Table 3). Two of these clasts have high MgO contents—73215,580 (,539/,563/,7002) at 40.8 wt% and 77035,226 (,172/,7001) at 49 wt%. These MgO-rich clasts have the lowest Na, K, Ca, and Al contents of the clasts analyzed (Ti was below detection limit) in each case. The remaining clasts are Al rich, containing >23 wt% Al_2O_3.

Trace-element chemistry of the melt-free clasts is variable, as expected from the petrography. The two "dunites" have higher abundances of incompatible trace elements (ITEs) and lower compatible-trace-element abundances than the Apollo dunite 72415 (Fig. 2A). Dunite 77035,226 generally follows the profile for the Mg-rich troctolite 76535 (Fig. 2A), but displays a large negative Eu anomaly [$(Eu/Eu^*)_N$ = 0.05]. Positive anomalies at Ta and Hf (however, see above) are present in this sample and the heavy rare-earth elements are elevated relative to 76535. Dunite 73215,580 has a similar pattern to 77035,206, although the negative Eu anomaly is not as pronounced [(Eu/Eu*)N = 0.51].

Gabbronoritic anorthosite 73216,66 (,36/,61/,7001) possesses a chondrite-normalized trace-element profile very similar to the Mg-rich norite 77215 (Fig. 2B), even though breccia matrix was seen in the thin section prepared from the INAA sample (73216,7001). Gabbronoritic anorthosite 73216,70 (,57/,65/,7005), anorthositic gabbronorite 77035,206 (,206), and gabbroic anorthosite 77035,229 (,200/,7003) have similar chondrite-normalized trace-element profiles that are parallel to ,66 with overall lower abundances. The final clast in this group is that of granulitic clast 73215,579 (,534/,562/,7001), which has essentially the same trace-element abundances and chondrite-normalized trace-element profile as that of Mg-rich troctolite 76535 (Fig. 2B). Iridium was only detected in two samples—73216,70 (,57/,65/,7005) and 77035,206 (,206). The presence of 15 ppb Ir in 73216,70 is surprising, inasmuch as the clast exhibits a striking cumulate texture, and no adhering breccia matrix was observed in the thin section made from the INAA sample. 77036,206 contains 37 ppb Ir, but has an overall granoblastic to granulitic texture, indicative of disruption by meteorite impact.

Melt-rich clasts

Six of the 13 clasts studied are either impact melts (73216,68; 77035,227; 77035,228) or contain melt of presumed impact origin as crosscutting veins (73216,67; 73216,69; 77035,230). Five of these clasts contain the highest K_2O abundances (0.24 to 0.39 wt%) of the clasts analyzed (Fig. 1E; Table 3), and four have the highest TiO_2

TABLE 3. Whole-Rock Compositions[1]

Breccia:	73215	77035	73215	77035	73216	73216	73216	77035
INAA no.:	,579	,206	,580	,226	,66	,70	,229	,230
Section no.:	,534/,562	,206	,539/,563	,172	,36/,61	,57/,65	,200	,201
Rock type:	Sp. troct.	Troctolite	Dunite	Dunite	Anorth.	Anorth.	Anorth.	Anorth.
Weight (mg):	30.0	68.4	43.4	27.2	27.5	72.9	19.4	13.3
				wt%				
TiO_2	n.d.	0.22	n.d.	n.d.	0.66	0.23	0.69	0.68
Al_2O_3	28.1	23.9	6.12	0.28	28.2	27.7	27.4	32.1
FeO	2.13	5.80	8.70	11.0	3.40	2.67	3.9	2.00
MnO	0.03	0.07	0.09	0.12	0.04	0.04	0.05	0.03
MgO	9.40	7.90	40.8	49.0	3.3	4.2	5.9	4.8
CaO	14.2	14.6	3.4	n.d.	15.9	17.5	14.2	18.2
Na_2O	0.40	0.43	0.12	0.02	0.64	0.39	1.21	0.55
K_2O	0.05	0.08	0.03	n.d.	0.14	0.03	0.18	0.32
Mg#	89	71	89	89	63	74	73	81
				ppm				
Sc	2.9	9.4	3.4	5.6	8.9	5.3	3.0	5.0
V	28	29	27	25	25	15	17	19
Cr	2080	810	1010	510	660	390	440	300
Co	13.1	41	55	62	20.1	5.8	5.8	4.3
Ni	120	560	420	110	170	60	n.d.	35
Sr	180	180	n.d.	n.d.	200	190	410	200
Ba	28	110	52	n.d.	170	80	130	240
Rb	n.d.	n.d.	n.d.	n.d.	4	n.d.	n.d.	9
Cs	n.d.	n.d.	n.d.	n.d.	n.d.	n.d.	n.d.	0.32
La	1.69	5.1	3.4	1.28	13.1	4.3	4.5	18.1
Ce	3.9	14.1	9.8	3.5	35	11.1	11.3	47
Nd	n.d.	7.5	4.9	3.4	19	6.8	6.7	29
Sm	0.83	2.27	1.61	1.38	5.8	1.98	1.81	7.7
Eu	0.7	0.96	0.28	0.026	1.49	1.18	3.19	1.58
Tb	0.19	0.59	0.32	0.3	1.22	0.45	0.38	1.6
Dy	0.98	3.4	2.4	1.8	7.5	2.8	2.7	11
Yb	0.5	2.12	1.18	1.18	4	1.55	1.09	4.8
Lu	0.075	0.31	0.174	0.2	0.53	0.23	0.16	0.66
Hf	0.35	1.72	1.39	0.44	3.4	1.02	0.9	5.2
Ta	n.d.	0.2	n.d.	1.7	0.55	0.13	0.19	0.76
Th	0.2	0.93	0.62	0.33	1.53	0.45	0.47	2.7
U	n.d.	0.2	0.17	n.d.	0.42	n.d.	n.d.	0.8
				ppb				
Ir	n.d.	37	n.d.	n.d.	n.d.	15	n.d.	n.d.
Au	4	11	8	6	8	11	6	15
$(La/Yb)_N$	2.26	1.61	1.93	0.73	2.19	1.86	2.76	2.52
$(Eu/Eu^*)_N$	2.38	1.15	0.51	0.05	0.74	1.69	5.10	0.60

(continued)

contents (Fig. 1C; Table 3). The impact melt 77035,228 (,185/,221/,7002) contains the lowest K_2O contents (0.11 wt%) of the analyzed melt rocks. The melt-rich clasts are generally moderate to low Mg (<12 wt% MgO; Fig. 1; Table 3). Apart from the generally elevated K_2O and TiO_2 contents, the melt-rich clasts have major-element compositions similar to those of the melt-free clasts (Fig. 1).

The chondrite-normalized trace-element profiles of the six melt-rich clasts are essentially subparallel to each other and the field for Apollo 17 KREEP basalts (Fig. 2C), although the negative Sr anomaly exhibited by the KREEP basalts is not

TABLE 3. (*continued*)

Breccia:	73216	73216	77035	73216	77035	
INAA no.:	,67	,68	,227	,69	,228	
Section no.:	,38/,62	,42/,63	,227	,49	,185/,221	Uncertainty
Rock type:	Impact	Impact	Impact	Norite	Norite	%
Weight (mg):	98.3	124.1	43.1	110.5	45.6	
			wt%			
TiO_2	1.7	1.45	1.48	1.32	0.21	10–30
Al_2O_3	17.8	21.8	17.1	15.3	19.7	<5
FeO	7.9	4.4	8.4	8.9	5.8	<2
MnO	0.10	0.06	0.11	0.13	0.09	<2
MgO	10.2	7.0	11.7	13.3	11.9	5–15
CaO	11.9	14.7	9.7	9.7	12.2	5–10
Na_2O	0.71	0.75	0.65	0.57	0.46	<2
K_2O	0.36	0.39	0.30	0.24	0.11	10–30
Mg#	70	74	71	73	79	
			ppm			
Sc	17.5	9.8	15.7	17.7	10.1	<2
V	41	27	40	43	64	10–20
Cr	1260	700	1170	1500	1950	<5
Co	20.8	8.2	38	18.6	21.4	<5
Ni	190	80	300	160	26	5–25
Sr	220	270	240	140	160	10–20
Ba	390	430	350	320	100	10–25
Rb	12	13	12	8	4	10–30
Cs	0.43	0.42	0.34	0.26	0.40	10–25
La	34	35	33	29	7	<5
Ce	89	89	81	73	17.8	2–15
Nd	50	49	48	40	11.3	5–15
Sm	15.2	14.1	14.8	12.6	2.89	<5
Eu	1.96	2.42	1.78	1.68	1.10	2–10
Tb	3.3	2.6	3.3	2.6	0.65	5–15
Dy	19	18	19	17	4.1	5–10
Yb	10.7	8.3	10.3	9.7	2.5	2–10
Lu	1.45	1.08	1.19	1.35	0.37	2–10
Hf	12.4	10.0	12.8	9.6	1.71	2–10
Ta	1.92	1.49	1.44	1.32	0.24	5–10
Th	5.3	4.8	5.3	4.4	1.38	2–10
U	1.5	1.4	1.5	1.3	0.29	10–20
			ppb			
Ir	5	n.d.	n.d.	n.d.	n.d.	5–25
Au	4	8	9	5	5	5–20
$(La/Yb)_N$	2.12	2.82	2.14	2.00	1.87	
$(Eu/Eu^*)_N$	0.37	0.51	0.34	0.39	1.08	

[1]Abbreviations: n.d. = not detected; Sp. tract. = spinel troctolite; Anorth. = anorthosite; Impact = impact melt.

as exaggerated in these clasts. Furthermore, the compatible trace elements are more fractionated relative to the highly incompatible trace elements (ITEs) compared to Apollo 17 KREEP (Fig. 2C). Higher ITE abundances generally are positively correlated with higher K_2O contents (Table 3). Impact melt 77035,228 (,185/,221/,7002) contains the lowest abundances of ITEs of these melt-rich clasts, but has the highest compatible-element abundances and has a chondrite-

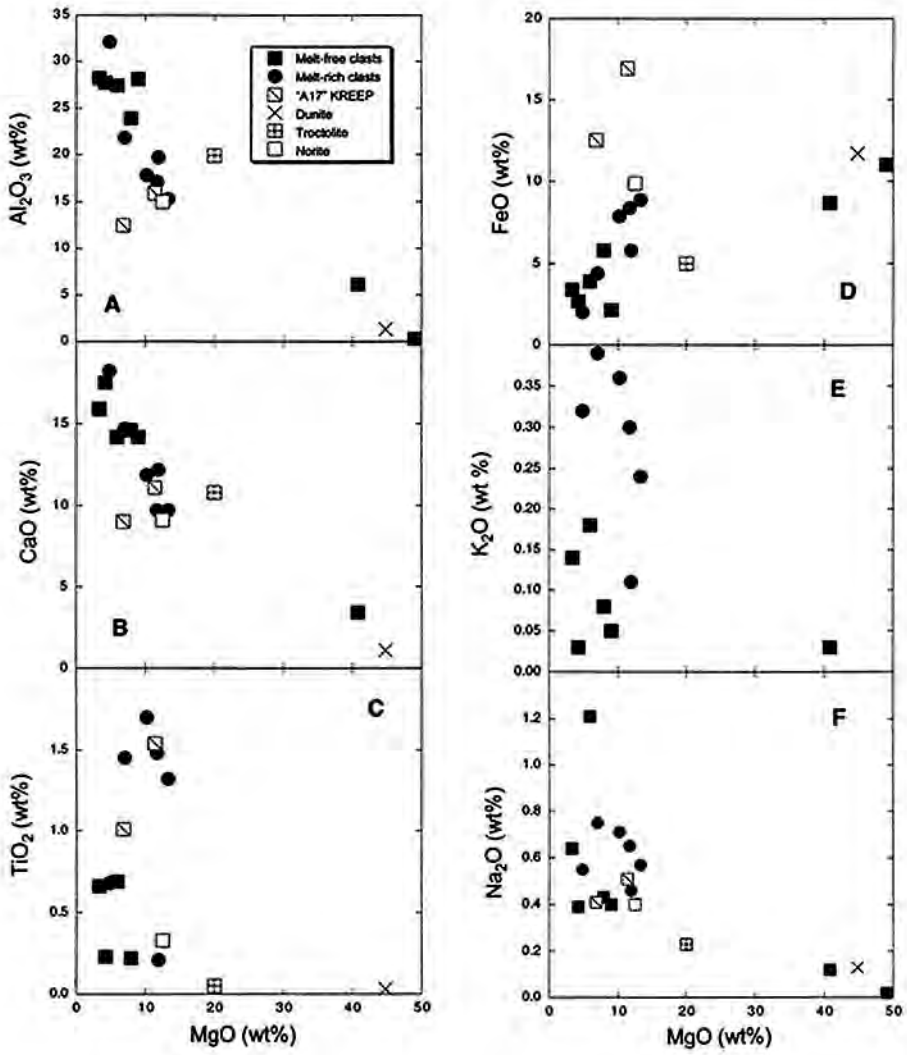

FIG. 1. Major-element chemistry for the 13 new Apollo 17 breccia clasts.

normalized trace-element profile quite similar to that of Mg-rich norite 77215 (Fig. 2C). Iridium was only detected in 73216,67 (5 ppb, Table 3).

Classification and modal mineralogy

These Apollo 17 highland samples have been classified as being derived primarily from the Mg-suite on the basis of An content and mafic mineral Mg#. Impact-melt clasts have not been classified in this way. Modal mineralogy of the seven melt-free clasts was determined using major- and minor-element whole-rock and average mineral data (Table 4). The mineral proportions were varied to produce a "best fit." Where a good fit (i.e., <10% deviation for most elements) was observed, we concluded that the resulting mode represents the mineral proportions in the INAA whole-rock sample. This produces consistent results and is preferable to point counting on the thin section made from the INAA sample; the samples are small, and the point-counted mode may not represent the whole-rock sample analyzed because material is lost in the sectioning procedure. Modes were not calculated for the melt-rich clasts be-

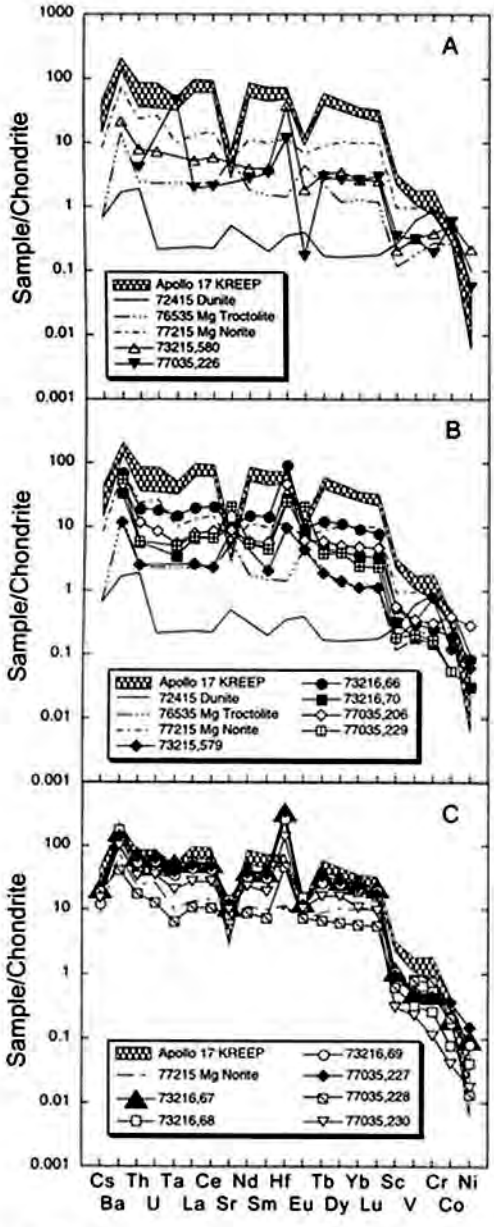

FIG. 2. Chondrite-normalized trace element patterns of (A) dunitic clasts, (B) melt-free clasts, and (C) melt-rich clasts; 72415/7 dunite (Laul and Schmit, 1975; Ryder, 1992), 77215 Mg-norite (Winzer et al., 1974, 1977), and 76535 Mg-troctolite (Haskin et al., 1974; Rhodes et al., 1974; Weismann and Hubbard, 1975) are plotted for comparison. LKFM field from Wanke et al. (1976) and Vaniman and Papike (1980).

cause of the presence of opaque glassy impact melt as well as devitrified impact melt. The variable composition of this melt yielded unacceptable results when we attempted to calculate the mode from mineral and whole-rock compositions.

Discussion

New clasts: Melt-free

The Al-rich clast 73215,534/,562/,7001 (,579) is composed of two components—light and dark breccia matrix. The light matrix is granulitic in texture and dominated by plagioclase, and is similar to the granulitic breccia reported by Warner et al. (1977) and Lindstrom and Lindstrom (1986). The dark matrix is cataclastic to porphyroblastic, containing clasts of spinel, olivine, low-Ca pyroxene, and plagioclase set in a matrix dominated by fine-grained (<30 μm) mineral fragments and opaque glass. Although undoubtedly representing a mixture of two lithologies, whole-rock and mineral chemistries are similar to the troctolite 76535 (Haskin et al., 1974; Rhodes et al., 1974; Weismann and Hubbard, 1975), although the spinel is more aluminous (Cr/Cr + Al = 0.10 vs. 0.68).

By simple comparison with the spinel cataclasite assemblage of Warner et al. (1978), Neal, Taylor et al. (1990b) suggested that 73215,534/,562/,7001 (,579) was of deep-seated ($\leq$60 km) origin. According to the classification of Steele and Smith (1975), this is supported by the low CaO contents ($\approx$0.02 wt%) of the olivine. The CaO contents of olivine in this sample were analyzed using extended count times (60 seconds) for both peak and background determinations. The CaO content of the olivine is consistent with an origin for 73215,534/,562/,7001 (,579) at least as great as those of previously reported spinel troctolites and cataclasites (2–3 kbar, or up to 60 km) (Bence et al., 1974; Herzberg, 1978). However, the low CaO contents of olivine could result from crystallization history (Steele and Smith, 1975). This would require early crystallization of Ca-poor olivine from a melt prior to enrichment of the magma in CaO. The high plagioclase content of 73215,579(,534/,562) and its anorthite-rich character (An_{90-97}) argue against this. If low-Ca olivine and An-rich plagioclase were coprecipitated from a single magma, it would favor a high-pressure origin for the troctolitic anorthosites (Anderson, 1973; Bence et al., 1974).

TABLE 4. Calculated Modes (%) Using Mineral and Whole-Rock Major-Element Chemistries for Melt-Free Clasts Only

Clast	Olivine	Plag.	Opx	Cpx	Ilm.	Armal.	Spinel	Metal	Classification
					73215				
,534	20.0	76.0	1.0	1.0	—	—	2.0	—	Granulitic trocotolite
,539	81.0	17.0	1.0	1.0	—	—	tr.[1]	—	Dunite
					73216				
,36	7.6	85.0	3.1	3.1	1.2	—	—	tr.	Gabbronoritic anorthosite
,57	—	78.0	10.0	12.0	—	—	—	tr.	Gabbronoritic anorthosite
					77035				
,172	100.0	—	—	—	—	—	—	—	Dunite
,200	9.0	80.0	7.0	3.0	1.0	—	—	tr.	Gabbroic anorthosite
,206	10.0	66.0	10.9	13.0	0.1	—	—	tr.	Anorthositic gabbronorite

[1]tr = trace amounts present.

The two "dunites" [73215,580 (,530/,563/,7002) and 77035,226 (,172/,7001)] contain 40.8 wt% and 49.0 wt% MgO, respectively, but exhibit different trace-element characteristics, and 77035,226 (,172/,7001) contains minor plagioclase, clinopyroxene, and orthopyroxene. Furthermore, they are distinct from dunite 72415 in that the overall ITE abundances are enriched, and both display a negative Eu anomaly. Olivine in 77035,226 (,172/,7001) exhibits core-to-rim variation (Fo_{88-72}), as presumably does 73215,580 (,539/,563/,7002) (Fo_{74-92}), is similar to the zonation described by Ryder (1992) for 72415, and was interpreted as indicating relatively rapid cooling in a hyperbyssal environment. However, calculation of equilibrium liquid REE profiles (using the Kds of McKay, 1986) yields highly LREE-enriched compositions, with La abundances at 40,000 × chondrite levels. Either the Kds are not applicable, or the olivines cocrystallized with other minerals. The presence of deep negative Eu anomalies in these clasts suggests either derivation from a source with a negative Eu anomaly and/or crystallization with or after plagioclase. Generation of the negative Eu anomaly in 77035,226 (,172/,7001) by melting alone would require plagioclase in the residue, which is unlikely. On the basis of these observations, it can be concluded that these clasts probably are unrepresentative samples from a hypabyssal troctolitic parent. This would require generation of a parental melt that would precipitate olivine of Fo_{92} composition, which requires the source to have a Mg# greater than the accepted bulk Moon values of 80 to 84 (Jones and Delano, 1989; O'Neill, 1991). Hess (1994) demonstrated the difficulty of generating magmas with the required Mg# for olivine and allow co-precipitation of plagioclase to form the lunar magma ocean. Magmas with high Mg# are inherently undersaturated with respect to plagioclase, which does not appear on the liquidus prior to substantial olivine fractionation, which in turn leads to a substantial decrease in the Mg# of the magma (Hess, 1994). The high Mg# could be generated after melting by reduction of FeO to metallic Fe, but the generation of high Mg# olivines remains under debate.

Two gabbronoritic anorthosites exhibit apparent cumulate textures [73216,66 (,36/,61/,7001) and 73216,70 (,57/,65/,7005)], whereas gabbroic anorthosite 77035,229 (,200/,7003) and anorthositic gabbronorite 77035,206 (,206) have been heavily brecciated. 77035,206 (,206) contains 37 ppb Ir and 560 ppm Ni (Table 3), consistent with its brecciated texture, but 77035,229 (,200/,7003) does not contain detectable Ni or Ir. The apparently pristine gabbronoritic anorthosites also present a dichotomy in terms of siderophile elements in that 73216,66 (,36/,61/,7001) does not have detectable Ir and contains 170 ppm Ni, whereas 73216,70 (,57/,65/,7005) contains 15 ppb Ir, only 60 ppm Ni, and the INAA sample contained no adhering breccia matrix. The presence of significant Ir in pristine lunar rocks is not common, but neither is it unusual. For example, Warren et al. (1990) reported 19 ppb of Ir in magnesian harzburgite 12033,503; Morgan and

Wandless (1988) analyzed dunite 72451 ten times, yielding an average Ir abundance of 0.62 ppb; and Warren et al. (1987) reported 1.3 ppb Ir in a pristine ferroan anorthosite 15363,1. The new data reported here provide further evidence supporting the contention of Warren et al. (1987, 1990) that large uncertainties are associated with estimating the highly siderophile element composition of the lunar crust.

Chondrite-normalized trace-element patterns of these anorthositic clasts are very similar to one another and to the Mg-rich norite 77215 (Winzer et al., 1974, 1977), although 73216,66 (,36/,61/,7001) has elevated trace-element abundances relative to the other three clasts. Rare-earth-element profiles for equilibrium liquids have been calculated for the two pristine samples using calculated modes and partition coefficients for pigeonite (McKay et al., 1991), clinopyroxene (McKay et al., 1986), ilmenite (Nakamura et al. 1986), olivine (McKay, 1986), and plagioclase (Phinney and Morrison, 1990). The equilibrium REE profiles thus calculated for both 73216,66 (36/,61/,7001) and 73216,70 (,57/,65/,7005) are elevated above LKFM [low-K Fra Mauro KREEP component first defined by Reid et al. (1972) from impact-generated glasses present at the Apollo 15 site] and Apollo 17 KREEP (Fig. 3); this is surprising considering the primitive nature of the major elements. Both calculated equilibrium liquids exhibit a marked negative Eu anomaly, indicating they were probably derived from a source with an inherent negative Eu anomaly. The primitive mineralogy argues against the contention that these equilibrium liquids were the result of large degrees of fractional crystallization.

At least four possible scenarios may explain the calculated equilibrium liquid REE profiles: (1) the partition coefficients used in this study are inappropriate—this is unlikely inasmuch as they were chosen specifically because of their applicability to lunar systems; (2) the primitive parental liquid assimilated a portion of urKREEP, which radically altered the incompatible trace elements, but the primitive mineralogy was maintained (cf. Warren, 1985); (3) after solidification at depth within the lunar crust, the monomict lithologies were patently metasomatized by a KREEPy fluid (Neal and Taylor, 1989, 1991); or (4) the calculation of equilibrium liquid compositions is inapplicable because the products of two liquids are

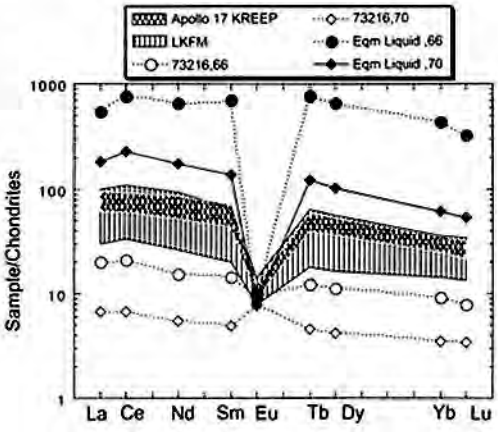

FIG. 3. Calculated equilibrium liquid REE patterns using literature Kds and calculated modes (see text for discussion). Apollo 17 KREEP from Salpas et al. (1987) and LKFM from Wanke et al. (1976) and Vaniman and Papike (1980).

encapsulated—the plagioclase primocrysts crystallized early and the inter-cumulus pyroxenes crystallized from a more evolved, late-stage melt. However, unless ion-microprobe or laser-ablation ICP-MS studies are carried out to determine the trace-element contents of individual phases, the interpretation of these proposed monomict clasts cannot be more specific.

Melt-rich clasts

These clasts cluster around KREEP on chondrite-normalized trace-element plots (Fig. 2C), although 77035,228 exhibits a profile similar to the Mg-norite 77215. As all these clasts contain relatively high K_2O contents (relative to the melt-free clasts; see Fig. 1E), this suggests that the impact melt(s) pervading or comprising these clasts is KREEPy in composition. The presence of a unique KREEP signature at the Apollo 17 site was reported by Salpas et al. (1987), so it is logical to assume that these clasts (and other impact melts) at the Apollo 17 site could contain this KREEP component if they were locally derived. However, this is not the case (Fig. 4), because the new clasts and other Apollo 17 impact melts appear to be LKFM in composition. This supports the conclusion of Ryder and Wood (1977) that LKFM is dominant in the impact-melt breccias from Apollo 17. The similarity of the chondrite-normalized profiles to each other and to Mg-norite 77215 suggests that the LKFM component de-

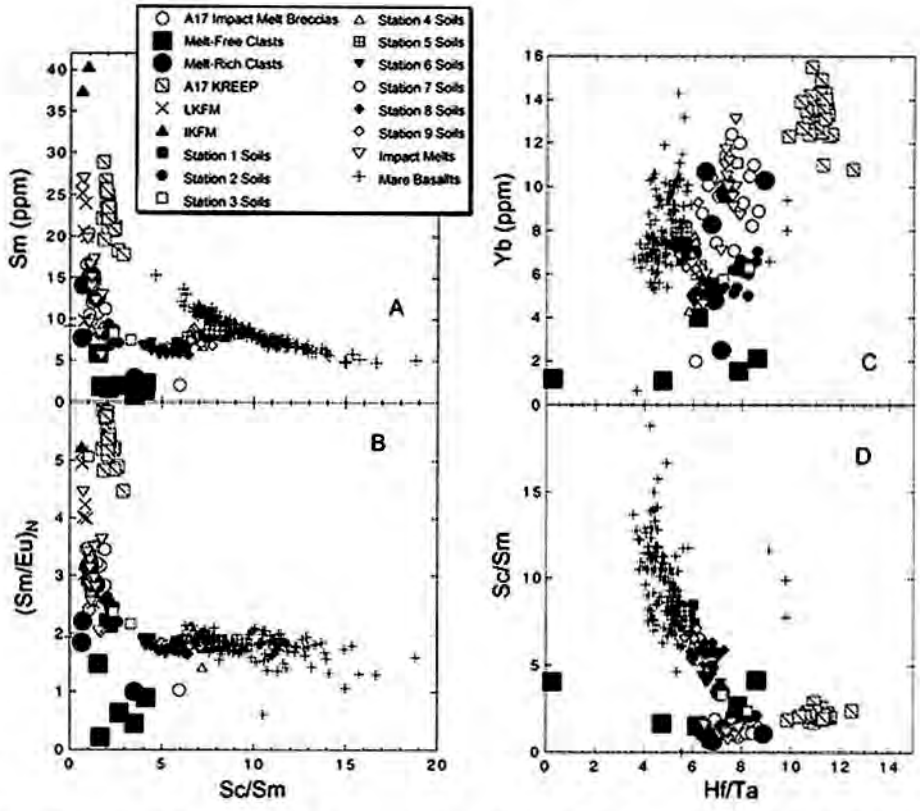

FIG. 4. Comparison of the 13 new Apollo 17 breccia clasts with other Apollo 17 lithologies. See text for discussion.

fined by these clasts is dominated by noritic rather than basaltic components (Ryder and Wood, 1977), although Ryder et al. (1997) suggested that evolved gabbroic lithologies also were important.

The bigger picture

Studies of the Serenitatis Basin have suggested that the Apollo 17 impact melt breccias were formed by the Serenitatis impact from locally derived materials (e.g., Spudis and Ryder, 1981; Dalrymple and Ryder, 1996), although Rockow and Haskin (1996) suggested that the evidence for this conclusion could be stronger. Ryder et al. (1997) concluded that the stratigraphy of this area was built up by complex and serial magmatism. This was dominated by Mg-suite lithologies at shallow depths with the deepest crust, sampled by the Serenitatis impact-melt breccias, being aluminous basalt in composition but consisting of a mixture of lithologies (including KREEP and evolved gabbroic rocks). By including the results of our small study into the bigger picture of the Serenitatis Basin, several interesting observations can be made regarding the petrology of the Apollo 17 site.

For this study, we have combined our data with those from other Apollo 17 breccia clasts (Laul et al., 1989), Apollo 17 impact melts and melt breccias (data compiled in Ryder, 1993, and Meyer, 1994), granulites (Warner et al., 1977; Lindstrom and Lindstrom, 1986), Apollo 17 mare basalts (Brunfelt et al., 1974; Shih et al., 1975; Warner et al., 1975a, 1975b, 1979; Rhodes et al., 1976; Murali et al., 1977; Neal, Paces et al., 1990; Neal, Taylor et al., 1990a; Ryder, 1990), and Apollo 17 soils (Korotev and Kremser, 1992), LKFM, and IKFM (Vaniman and Papike, 1980). This approach compares monomict and polymict rock and regolith samples from the Apollo 17 site in order to evaluate the significance of LKFM and Apollo 17 KREEP basalts in the Serenitatis Ba-

sin, and to qualitatively identify the major components involved in soil formation. We have not gone into the detail expended by Korotev and Kresmer (1992) to determine the components in the Apollo 17 soils; instead we use simple correlation plots to highlight what we feel are more appropriate components that will simplify the interpretation of soil components. It is beyond the scope of this modest study to evaluate whether the impact-melt breccias and clasts were derived from the Serenitatis impact or from further afield, although suggestions will be made as to possible origins.

Basic element–element plots (Figs. 5A and 5B) highlight some important features of the samples returned by the Apollo 17 mission. The soils reported by Korotev and Kresmer (1992)—who also included soils studied by Rhodes et al. (1974)—were interpreted to contain the following components—high-Ti and very low Ti mare basalts, orange pyroclastic glass, noritic breccia, anorthositic norite, and a meteorite component. Apollo 17 KREEP, defined by clasts from breccia 72275 (Salpas et al., 1987), was used only to describe soils from Station 2. The Apollo 17 soils span the gap between Apollo 17 mare basalts and highlands materials (Figs. 5A and 5B). However, it is evident from these simple element–element plots that the soils are not simple two-component mixtures between mare basalts and highlands. In Figures 5A and 5B, the trend defined by the soils leads from the mare basalt field (soils from Stations 1, 4, 5, and 9, which are all from the valley floor of the landing site) toward the region occupied by Apollo 17 highlands materials (soils from Stations 6, 7, and 8 at the base of the North Massif) before curving back toward a KREEPy component (soils from Stations 2 and 3 in the light-mantle area at the base of the South Massif).

However, this KREEPy component does not appear to be that defined by the KREEP basalt clasts in 72275. Rather, it is the enigmatic LKFM component, as defined by Apollo 16 samples (Vaniman and Papike, 1980), the Apollo 17 melt breccias and impact melts (see Ryder, 1993; Meyer, 1994), and the melt-rich clasts described in this study. This is further reinforced when the Sc/Sm ratio is plotted against Sm (ppm); in such diagrams, Apollo 17 impact lithologies, including the melt-rich clasts, plot with LKFM, which forms a trend parallel to the KREEP basalt clasts in

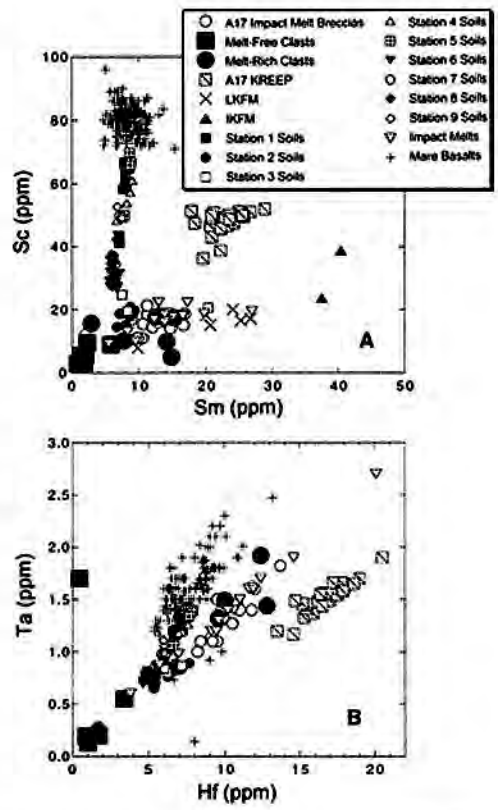

FIG. 5. Both (A) and (B) demonstrate that KREEPy lithologies at Apollo 17 are related to LKFM and not to the KREEP basalts found as clasts in breccia 72275 (Salpas et al., 1987). See text for discussion.

breccia 72275 (Fig. 6). Apollo 17 KREEP basalt is an inappropriate component for any of the Apollo 17 soils and impact lithologies. This is again emphasized by Figure 4(A–D), where Apollo 17 KREEP basalts form a distinct population from the Apollo 17 soils and the LKFM field. Furthermore, assuming the Apollo 17 soils are derived primarily from local materials, compositions suggest that the South Massif of the Apollo 17 landing site contains a larger proportion of KREEP ("LKFM" component and the KREEP basalts) than does the North Massif. We suggest that "Apollo 17" KREEP described by Salpas et al. (1987) from breccia 72275 is not derived from the Serenitatis Basin, but has been transported there by impact processes.

If 72275 KREEP basalt clasts are in fact foreign to the Serenitatis Basin, the predominance of LKFM must be explained, especially as it is found

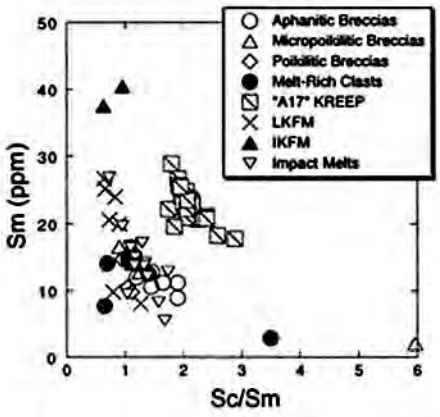

FIG. 6. Sc/Sm versus Sm (ppm) further demonstrates that the melt-rich clasts described in this study contain a KREEP component represented by LKFM, and are not related to 72275 KREEP basalts.

predominantly in impact-generated lithologies (Norman and Ryder, 1979; Norman et al., 1992). Reid et al. (1977) suggested that if the widespread occurrence of LKFM impact rocks could be related to a single major impact event, the likely candidate would be that which formed the Imbrium Basin. Alternatively, if the occurrence of LKFM rocks over large portions of the Moon was associated with several major impacts, it would argue for a significant portion of the lower lunar crust being composed of LKFM lithologies early in lunar history. Ryder and Wood (1977) argued that the anorthositic gabbro highlands are underlain by a layer of LKFM basalt up to 20 km thick.

It is evident from Figure 5B that LKFM impact lithologies are compositionally related to the lunar highlands. In this diagram, Apollo 17 LKFM impact melts and melt breccias, as well as the melt-rich clasts, have the same Hf/Ta ratio as highlands lithologies (here defined by the melt-free clasts). Hafnium-tantalum ratios will not be altered by fractional crystallization in a lunar environment, unless significant ilmenite is involved. This could mean that the Apollo 17 LKFM lithologies are composed of fractionated, Mg-suite highlands materials that were present at the top of Mg-suite plutons in the lunar crust (assuming simple, gravity-driven, fractional crystallization). These were ultimately mixed with more primitive cumulates lower in the pluton(s) materials by large impacts. The lack of ferroan anorthosite in the Apollo 17 LKFM lithologies has been reported previously (e.g., Norman et al., 1992; Ryder et al., 1997). Alternatively, the ubiquitous impact-generated LKFM compositions could be the result of large impacts exposing urKREEP (high-K) and mixing it with Mg-suite highlands lithologies at the Apollo 17 site. Exposure of KREEPy materials and mixing with more primitive components by large impacts explains the occurrence of LKFM as impact-generated glasses and breccias. However, one important conclusion for the Apollo 17 impact-generated LKFM lithologies is that their chemical composition cannot be supported from the lithic fragments they contain, requiring a "cryptic" component to be involved (Ryder, 1979). Ryder et al. (1997) concluded that a component akin to sodic ferrogabbro in breccia 67915 was present in the Serenitatis impact melts, and suggested that the LKFM component could be adequately described by a mixture of evolved gabbros and grabbronorites.

The cryptic components as defined in Ryder (1979) and Ryder et al. (1997), among others, are difficult to isolate. We suggest that this is because the KREEPy material, whether from the fractional crystallization of an Mg-suite pluton or the lunar magma ocean, represents material of the lowest melting point. This should represent the first material melted by any large impact, and thus will be present either as glass (e.g., Reid et al., 1972) or as microcrystalline breccia matrix. Therefore, definition of the mineralogy of this cryptic component will not be possible. Even if the KREEP component is not remobilized, it is probably present as a grain-boundary component between more primitive mineral grains. Inasmuch as it represents the last dregs of "Fenner-trend" fractional crystallization, it should be somewhat fluid in nature (Neal and Taylor, 1989) and subject to quenching as a glass, again making it difficult to define the cryptic component in LKFM lithologies.

Conclusions

This study has used mineralogy, petrography, and whole-rock chemistry to further explore the geology and evolution of the Serenitatis Basin. Integrating the 13 new clasts with previous studies of Apollo 17 samples, the following conclusions can be made.

1. Presence of 15 ppb Ir in 73216,70 (.571/.65/.7005) further demonstrates that large

uncertainties are associated with estimating the highly siderophile element content of the lunar crust, and siderophile-element abundances cannot be used in isolation to demonstrate pristinity, or lack thereof.

2. KREEP basalts from breccia 72275 probably are not indigenous to the Serenitatis Basin, and were transported to the Apollo 17 site by impact processes. Apollo 17 KREEP is, in reality, LKFM in composition.

3. The "cryptic" component required to define KREEPy LKFM impact compositions will probably never be defined mineralogically. This component is derived from the final liquid to crystallize from fractional crystallization of either an Mg-suite pluton or the lunar magma ocean. Consequently, this component will easily melt when disrupted by large impacts and is now present as glass in breccia matrixes and/or as grain boundary films.

Further studies are required in order to explore the origin of 72275 KREEP basalt clasts and to define the highly siderophile element budget of the lunar crust.

Acknowledgments

This research was funded by NASA grant NAG 9-415 to L. A. T. and would not have been possible without the initiative of Larry Taylor. Roman Schmitt is gratefully acknowledged for the INAA analyses and Allan Patchen for the electron-microprobe mineral analyses. Thoughtful reviews by Greg Snyder and an anonymous reviewer are gratefully acknowledged.

REFERENCES

Anderson, A. T., 1973, The texture and mineralogy of lunar peridotite 15445,20: Jour. Geol., v. 81, p. 219–226.

Bence, A. E., Delano, J. W., Papike, J. J., and Cameron, K. L., 1974, Petrology of the highlands massifs at Taurus-Littrow: An analysis of the 2–4 mm soil fraction: Proc. Lunar Sci. Conf., 5th, p. 785–827.

Blanchard, D. P., and Budahn, J. R., 1979, Remnants from the ancient lunar crust: Clasts from consortium breccia 73255: Proc. Lunar Planet. Sci. Conf., 10th, p. 803–816.

Blanchard, D. P., Jacobs, J. W., and Brannon, J. C., 1977, Chemistry of the ANT-suite and felsite clasts from consortium breccia 73215 and of gabbroic anorthosite 79215: Proc. Lunar Sci. Conf., 8th, p. 2507–2524.

Brunfelt, A. O., Heier, K. S., Nilssen, B., Steinnes, E., and Sundvoll, B., 1974, Elemental composition of Apollo 17 fines and rocks: Proc. Lunar Sci. Conf., 5th, p. 981–990.

Dalrymple, G. B., and Ryder, G., 1996, $^{40}Ar/^{39}Ar$ age spectra of Apollo 17 highlands breccia samples by laser step heating and the age of the Serenitatis basin: Jour. Geophys. Res., v. 101, p. 22,069–22,084.

Eckert, J. O., Taylor, L. A., and Neal, C. R., 1991a, Spinel troctolite from Apollo 17 breccia 73215: Evidence for petrogenesis as deep-seated lunar crust [abs.]: Lunar Planet. Sci., v. XXII, p. 329–330.

Eckert, J. O., Taylor, L. A., Neal, C. R., and Patchen, A. D., 1991b, Anorthosites with negative Eu anomalies in Apollo 17 breccias: Further evidence for "REEP" metasomatism [abs.]: Lunar Planet. Sci., v. XXII, p. 331–332.

Eckert, J. O., Taylor, L. A., Neal, C. R., Schmitt, R. A., Liu, Y.-G., and Patchen, A. D., 1991c, Cumulate lithologies and melt rocks from Apollo 17 breccias: Correlation of whole-rock and mineral chemistry [abs.]: Lunar Planet. Sci., v. XXII, p. 333–334.

Haskin, L. A., Shih, C.-Y., Bansal, B. M., Rhodes, J. M., Wiesmann, H., and Nyquist, L. E., 1974, Chemical evidence for the origin of 76535 as a cumulate: Proc. Lunar Sci. Conf., 5th, p. 1213–1225.

Herzberg, C. T., 1978, The bearing of spinel cataclasites on the crust-mantle structure of the Moon: Proc. Lunar Planet. Sci. Conf., 9th, p. 319–336.

Hess, P. C., 1994, Petrogenesis of lunar troctolites: Jour. Geophys. Res., v. 99, p. 19,083–19,093.

Hughes, S. S., Delano, J. W., and Schmitt, R. A., 1988, Apollo 15 yellow-brown glass: Chemistry and petrogenetic relations to green glass and olivine-normative mare basalts: Geochim. et Cosmochim. Acta, v. 52, p. 2379–2391.

James, O. B., Brecher, A., Blanchard, D. P., Jacobs, J. W., Brannon, J. C., Korotev, R. L., Haskin, L. A., Higuchi, H., Morgan, J. W., Anders, E., Silver, L. T., Marti, K., Braddy, D., Hutcheon, I. D., Kirsten, T., Kerridge, J. F., Kaplan, I. R., Pillinger, C. T., and Gardiner, L. R., 1975, Consortium studies of matrix of light gray breccia 73215: Proc. Lunar Sci. Conf., 6th, p. 547–577.

James, O. B., and Hammarstrom, J. G., 1977, Petrology of four clasts from consortium breccia 73215: Proc. Lunar Sci. Conf., 8th, p. 2459–2494.

James, O. B., and McGee, J. J., 1980, Petrology of mare-type basalt clasts from consortium breccia 73255: Proc. Lunar Planet. Sci. Conf., 11th, p. 67–86.

Jones, J. H., and Delano, J. W., 1989, A three-component model for the bulk composition of the Moon: Geochim. et Cosmochim. Acta, v. 53, p. 513–527.

Korotev, R. L., and Kremser, D. T., 1992, Compositional variations in Apollo 17 soils and their relationship to the geology of the Taurus-Littrow site: Proc. Lunar Planet Sci. Conf., 22nd, p. 275–301.

Laul, J. C., Gosselin, D. C., Galbreath, K. C., Simon, S. B., and Papike, J. J., 1989, Chemistry and petrology of Apollo 17 highland coarse fines: Plutonic and melt rocks: Proc. Lunar Planet. Sci. Conf., 19th, p. 85–97.

Laul, J. C., and Schmitt, R. A., 1975, Dunite 72417: A chemical study and interpretation: Proc. Lunar Sci. Conf., 6th, p. 1231–1254.

Lindstrom, M. M., and Lindstrom, D. J., 1986, Lunar granulites and their precursor anorthositic norites of the early lunar crust: Proc. Lunar Planet. Sci. Conf., 16th, *in* Jour. Geophys. Res., v. 91, p. D263–D276.

McKay, G. A., 1986, Crystal/liquid partitioning of REE in basaltic systems: Extreme fractionation of REE in olivine: Geochim. et Cosmochim. Acta, v. 50, p. 69–79.

McKay, G. A., Wagstaff, J., and Le, L., 1991, REE distribution coefficients for pigeonite: Constraints on the origin of the mare basalt europium anomaly, III, *in* Mare Volcanism and Basalt Petrogenesis Workshop: LPI Tech. Rpt., 91–03, p. 27–28.

McKay, G. A., Wagstaff, J., and Yang, S.-R. 1986, Clinopyroxene REE distribution coefficients for shergottites: The REE content of the Shergotty melt: Geochim. et Cosmochim. Acta, v. 50, p. 927–937.

Meyer, C., 1994, Catalog of Apollo 17 rocks, v. 4: North Massif: Houston, Johnson Space Center JSC #26088, Office of the Curator #87.

Morgan, J. W., and Wandless, G. A., 1988, Lunar dunite 72415–72417: Siderophile and volatile trace elements [abs.]: Lunar Planet. Sci., v. XIX, p. 804–805.

Murali, A. V., Ma, M.-S., Schmitt, R. A., Warner, R. D., Keil, K., and Taylor, G. J., 1977, Chemistry of 30 Apollo 17 rake basalts: 71597 a product of partial olivine accumulation [abs.], *in* Lunar Sci., v. VIII, p. 703–705.

Nakamura, Y., Fujimaki, H., Nakamura, N., Tatsumoto, M., McKay, G. A., and Wagstaff, J., 1986, Hf, Zr, and REE partition coefficients between ilmenite and liquid: Implications for lunar petrogenesis: Proc. Lunar Planet. Sci. Conf., 16th, *in* Jour. Geophys. Res., v. 91, p. D239–D250.

Neal, C. R., Paces, J. B., Taylor, L. A., Hughes, S. S., and Schmitt, R. A., 1990a, Two new type C basalts: Petrogenetic implications for source evolution and magma genesis at the Apollo 17 site: Lunar Planet. Sci., v. XXI, p. 855–856.

Neal, C. R., and Taylor, L. A., 1989, Metasomatic products of the lunar magma ocean: The role of KREEP dissemination: Geochim. et Cosmochim. Acta, v. 53, p. 529–541.

———, 1991, Evidence for metasomatism of the lunar highlands and the origin of whitlockite: Geochim. et Cosmochim. Acta, v. 55, 2965–2980.

Neal, C. R., Taylor, L. A., Hughes, S. S., and Schmitt, R. A., 1990a, The significance of fractional crystallization in the petrogenesis of Apollo 17 type A and B high-Ti basalts: Geochim. et Cosmochim. Acta, v. 54, p. 1817–1833.

Neal, C. R., Taylor, L. A., and Patchen, A. D., 1990b, An Apollo 17 safari: Exciting new clasts from breccia "pull-apart" efforts [abs.]: Lunar Planet. Sci., v. XXI, p. 859–860.

Norman, M. D., and Ryder, G., 1979, A summary of the petrology and geochemistry of pristine highland rocks: Proc. Lunar Planet. Sci. Conf., 10th, p. 531–559.

Norman, M. D., Taylor, G. J., Spudis, P., and Ryder, G., 1992, Lithologies contributing to the clast population in Apollo 17 LKFM basaltic impact melts, *in* Ryder, G., et al., eds. Workshop on the Geology of the Apollo 17 Landing Site: LPI Tech. Report 92–09, pt. 1, p. 42–44.

O'Neill, H. St. C., 1991, The origin of the Moon and the early history of the Earth—A chemical model, part 1, The Moon: Geochim. et Cosmochim. Acta, v. 55, p. 1135–1157.

Phinney, W. C., and Morrison, D. A., 1990, Partition coefficients for calcic plagioclase: Implications for Archean anorthosites: Geochim. et Cosmochim. Acta, v. 54, p. 1639–1654.

Reid, A. M., Duncan, A. R., and Richardson, S. H., 1977, In search of LKFM: Proc. Lunar Sci. Conf., 8th, p. 2321–2338.

Reid, A. M., Warner, J., Ridley, W. I., and Brown, R. W., 1972, Major-element compositions of glasses in three Apollo 15 soils: Meteoritics, v. 7, p. 1127–1148.

Rhodes, J. M., Hubbard, N. J., Wiesmann, H., Rodgers, K. V., Brannon, J. C., and Bansal, B. M., 1976, Chemistry, classification, and petrogenesis of Apollo 17 mare basalts: Proc. Lunar Sci. Conf., 7th, p. 1467–1489.

Rhodes, J. M., Rodgers, K. V., Shih, C.-Y., Bansal, B. M., Nyquist, L. E., Wiesmann, H., and Hubbard, N. J., 1974, The relationships between geology and soil chemistry at the Apollo 17 landing site: Proc. Lunar Sci. Conf., 5th, p. 1097–1133.

Rockow, K. M., and Haskin, L. A., 1996, Why are Apollo 17 impact-melt breccias assigned a Serenitatis origin: A brief critical review: Lunar Planet. Sci., v. XXVII, p. 1089–1090.

Ryder, G., 1979, The chemical components of highlands breccias: Proc. Lunar Planet. Sci. Conf., 10th, p. 561–581.

———, 1990, A distinct variant of high-titanium mare basalt from the Van Serg core, Apollo 17 landing site: Meteoritics, v. 25, p. 249–258.

———, 1992, Chemical variation and zoning of olivine in lunar dunite 72415: Near-surface accumulation: Proc. Lunar Planet. Sci., 22nd, p. 373–380.

———, 1993, Catalog of Apollo 17 Rocks, v. 1: Stations 2 & 3 (South Massif). Houston, Johnson Space Center JSC #26088, Office of the Curator #87.

Ryder, G., Norman, M. D., and Taylor, G. J., 1997, The complex stratigraphy of the highland crust in the Serenitatis region of the Moon inferred from mineral-

fragment chemistry: Geochim. et Cosmochim. Acta, v. 61, p. 1083–1105.

Ryder, G., Stoeser, D. B., Marvin, U. B., and Bower, J. F., 1975, Lunar granites with unique ternary feldspars: Proc. Lunar Sci. Conf., 6th, p. 435–449.

Ryder, G., and Wood, J. A., 1977, Serenitatis and Imbrium impact melts: Implications for large-scale layering in the lunar crust: Proc. Lunar Sci. Conf., 8th, p. 655–668.

Salpas, P. A., Lindstrom, M. M., and Taylor, L. A., 1988, Highland materials at Apollo 17: Contributions from 72275: Proc. Lunar Planet. Sci. Conf., 18th, p. 11–20.

Salpas, P. A., Taylor, L. A., and Lindstrom, M. M., 1987, Apollo 17 KREEPy basalts: Evidence for nonuniformity of KREEP: Proc. Lunar Planet. Sci. Conf., 17th, *in* Jour. Geophys. Res., v. 92, p. E340–E348.

Shih, C.-Y., Haskin, L. A., Wiesmann, H., Bansal, B. M., and Brannon, J. C., 1975, On the origin of high-Ti mare basalts: Proc. Lunar Sci. Conf., 6th, p. 1255–1285.

Smith, J. V., Anderson, A. T., Newton, R. C., Olsen, E. J., Wyllie, P. J., Crewe, A. V., Isaacson, M. S., and Johnson, D., 1970, Petrologic history of the Moon inferred from petrography, mineralogy, and petrogenesis of Apollo 11 rocks: Proc. Apollo 11 Lunar Sci. Conf., p. 897–925.

Spudis, P. D., and Ryder, G., 1981, Apollo 17 impact melts and their relation to the Serenitatis Basin, in Schultz, P. H., and Merrill, R. B., eds., Multi-ring basins: Proc. Lunar Planet Sci. Conf., v. 12A, p. 133–148.

Steele, I. M., and Smith, J. V., 1975, Minor elements in lunar olivine as a petrologic indicator: Proc. Lunar Sci. Conf., 6th, p. 451–467.

Taylor, S. R., and Jakes, P., 1974, The geochemical evolution of the Moon: Proc. Lunar Sci. Conf., 5th, p. 1287–1305.

Vaniman, D. T., and Papike, J. J., 1980, Lunar highland melt rocks: Chemistry, petrology, and silicate mineralogy, *in* Papike, J. J., and Merrill, R. B., eds. Proc. Conf. Lunar Highlands Crust, p. 271–338.

Wanke, H., Palme, H., Kruse, H., Baddenhausen, H., Cendales, M., Dreibus, G., Hofmeister, H., Jagoutz, E., Palme, C., Spettel, B., and Thacker, R., 1976, Chemistry of lunar highland rocks: A refined evaluation of the composition for the primary matter: Proc. Lunar Sci. Conf., 7th, p. 3479–3499.

Warner, J. L., Phinney, W. C., Bickel, M. E., and Simonds, C. H., 1977, Feldspathic granulitic impactites and pre-final bombardment lunar evolution: Proc. Lunar Sci. Conf., 8th, p. 2051–2066.

Warner, R. D., Keil, K., Murali, A. V., and Schmitt, R. A., 1975a, Petrogenetic relationships among Apollo 17 basalts [abs.], *in* Papers to the Conf. on Origins of Mare Basalts and Their Implications for Lunar Evolution, Lunar Science Institute, Houston, p. 179–183.

Warner, R. D., Keil, K., Prinz, M., Laul, J. C., Murali, A. V., and Schmitt, R. A., 1975b, Mineralogy, petrology, and chemistry of mare basalts from Apollo 17 rake samples: Proc. Lunar Sci. Conf., 6th, p. 193–220.

Warner, R. D., Taylor, G. J., Conrad, G. H., Northrop, H. R., Barker, S., Keil, K., Ma, M.-S., and Schmitt, R. A., 1979, Apollo 17 high-Ti mare basalts: New bulk compositional data, magma types, and petrogenesis: Proc. Lunar Planet. Sci. Conf., 10th, p. 225–247.

Warner, R. D., Taylor, G. J., Mansker, W. L., and Keil, K., 1978, Clast assemblages of possible deep-seated (77517) and immiscible-melt (77538) origins in Apollo 17 breccias: Proc. Lunar Planet. Sci. Conf., 9th, p. 941–958.

Warren, P. H., 1985, The magma ocean concept and lunar evolution: Ann. Rev. Earth Planet. Sci., v. 13, p. 201–240.

Warren, P. H., Jerde, E. A., and Kallemeyn, G. W., 1987, Pristine Moon rocks: A "large" felsite and a metal-rich ferroan anorthosite: Proc. Lunar Planet. Sci. Conf., 17th, *in* Jour. Geophys. Res., v. 92, p. E303–E313.

———, 1990, Pristine Moon rocks: An alkali anorthosite with coarse augite exsolution from plagioclase, a magnesian harzburgite, and other oddities: Proc. Lunar Planet. Sci. Conf., 20th, p. 31–59.

———, 1991, Pristine Moon rocks: Apollo 17 anorthosites: Proc. Lunar Planet. Sci. Conf., 21st, p. 51–61.

Wiesmann, H., and Hubbard, N. J., 1975, A compilation of the lunar sample data generated by the Gast, Nyquist, and Hubbard lunar PI-ships: Unpubl. manuscript.

Winzer, S. R., Nava, D. F., Schuhmann, S., Kouns, C. W., Lum, R. K. L., and Philpotts, J. A., 1974, Major, minor, and trace-element abundances in samples from Apollo 17 Station 7 boulder: Implications for the origin of early lunar crustal rocks: Earth Planet. Sci. Lett., v. 23, p. 439–444.

Winzer, S. R., Nava, D. F., Schuhmann, S., Lum, R. K. L., Lindstrom, M. M., Lindstrom, D. J., and Philpotts, J. A., 1977, The Apollo 17 "melt sheet": Chemistry, age, and Rb/Sr systematics: Earth Planet Sci. Lett., v. 33, p. 389–400.